Journal of Aircraft

VOLUME 7 SEPTEMBER-OCTOBER 1970 NUMBER 5

Journal Users—Send Your Comments on SYNOPTICS

Several sample *Synoptics* have appeared in the August, September, and September-October issues of the Journals. The Publications Committee will discuss the implementation of *Synoptics* into the Journal structure at its October meeting. *Please send your suggestions or comments (positive or negative)* to Dr. Jerry Grey, Vice-President, Publications, at AIAA, 1290 Sixth Avenue, New York, N.Y. 10019 *prior to October 5* so that the Publications Committee will be able to consider your views in its deliberations.

Aerodynamic Design Integration of Supersonic Aircraft

DONALD D. BAALS, A. WARNER ROBINS, AND ROY V. HARRIS JR.

NASA Langley Research Center, Hampton, Va.

Introduction

MOST of the basic theories of supersonic flow were developed in the late 1940's and early 1950's. Many of these theories were very complex and could be applied only to simple classical examples with few practical applications to be found in the design of real airplanes. More recently, however, the availability of high-speed digital computers has brought about a revolution in the use of aerodynamic theory. Many of the theories which once were considered too complex can now be used to optimize the design and assess the performance characteristics of complex, real airplane configurations.

During the past decade, a small group at the NASA Langley Research Center has become the focal point for coordinating

Donald D. Baals is a native of Fort Wayne, Ind., graduated from Purdue University in 1938 and received his M.S. degree in 1939. He joined the staff of the NACA (now NASA) Langley Research Center in 1939 and conducted fundamental research in the area of air inlets and transonic flows. He designed the Langley 4-ft supersonic pressure tunnel and was one of the architects of the National Unitary Plan facilities program. He has been a key member of the Langley aeronautical research effort and has published over 30 technical reports and papers in the areas of inlet aerodynamics, wing variable sweep, high cruise efficiency aircraft, and sonic boom. For the past decade, he has directed research in support of the supersonic transport and has been closely identified with the National SST Program. He is an Associate Fellow of the AIAA, a member of the NASA Subcommittee on Aircraft Aerodynamics, and a member of the AIAA Technical Committee on Aircraft Design. He is currently Assistant Chief of the Full-Scale Research Division at the NASA Langley Research Center.

Warner Robins, a former military pilot, received his B.S. degree from the Virginia Polytechnic Institute in 1949. He immediately joined the staff of the Langley Research Center where he has been very active since in experimental and analytical research in supersonic aerodynamics. He is currently Assistant Head of the Large Supersonic Tunnels Branch of the Langley Research Center.

Roy Harris is a native of Augusta, Ga., whose aviation experience began as a flight-line attendant and includes that of aircraft owner, "crop-duster" pilot, flight instructor, commercial pilot, and Air Force officer. He was graduated from the Georgia Institute of Technology in 1958 with a B.S. degree in aeronautical engineering, and immediately joined the NACA (now NASA) Langley Research Center staff as a research engineer. Since that time, he has served as project engineer on many experimental and theoretical investigations in supersonic aerodynamics, and has authored more than 24 technical reports and papers. As a result of his research work, he was awarded the AIAA Lawrence Sperry Award for 1968. He is a Member of AIAA.

Presented as Paper 68-1018 at the AIAA 5th Annual Meeting and Technical Display, Philadelphia, Pa., October 21–24, 1968; submitted December 16, 1968; revision received February 13, 1970.

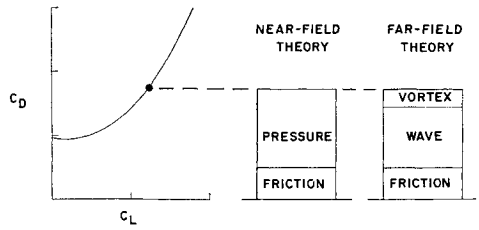

Fig. 1 Theoretical drag estimation methods.

and extending the basic supersonic theories, for programing these analytical procedures for high-speed digital computers, and for providing experimental determination of the applicability and limitations of these new aerodynamic design tools. The result of this work has been a relatively sophisticated complex of computer programs, many of which have been adopted by the aircraft industry. This work has had a profound effect on modern aircraft design, especially the supersonic transport, and is finding growing application to the design integration of supersonic military aircraft and missiles. Substantial progress has also taken place in the application of subsonic theories, as well as in the area of computer-aided structural design. The present paper will be limited, however, to supersonic aerodynamic considerations only and will review the more commonly used theories, describe the numerical solutions that are used in the Langley computer complex, and illustrate the use of the programs in the design of an illustrative supersonic transport (SST) configuration.

The two basic theoretical methods that can be used to analyze the lift-drag characteristics of an airplane at supersonic speeds are illustrated in Fig. 1. The first might be called a near-field theory and involves the calculation of local pressures on the three-dimensional surfaces of the airplane. Because of the complexity of these calculations, early attempts to use the near-field approach have been limited to thin wings or simple wing-body combinations.[1,2] More recent numerical methods for applying this approach show promise of extending the near-field approach in the future to include the more complex, real-airplane shapes.[3]

The second is a far-field theory and involves momentum considerations across the surfaces of a very large cylindrica control volume that encompasses the airplane. This approach can be used with present methods to calculate the wave drag of complex, real-airplane shapes. However, in the far-field, the invicsid drag consists of both wave and vortex components, and the pure far-field approach is limited by the absence of a satisfactory numerical method for including the effects of leading-edge suction on the vortex drag. In both of these theoretical methods,the viscous skin-friction drag can be treated separately, and adequately evaluated by strip integration over the aircraft surfaces.

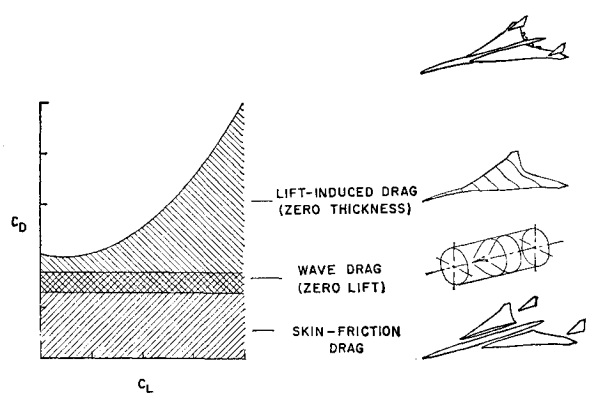

Fig. 2 Illustration of hybrid theoretical approach.

The most commonly used method of analysis, and the one considered in this paper, involves a hybrid approach that combines the near-field and far-field methods in a particular manner such that complex, real-airplane shapes can be analyzed. This approach is illustrated in Fig. 2. In this approach, the inviscid drag is accounted for by combining near-field theory at zero thickness and far-field theory at zero lift. Then the thickness effects (wave drag) can be separated from the lift effects and each handled by a theoretical approach for which present numerical methods are applicable to complex, real-airplane configurations.

Development of the Theory

Zero-Lift Wave Drag

Although supersonic theories have long been available to calculate the wave drag of slender bodies of revolution[4] and of thin wings,[5] it was not until 1952 when Whitcomb experimentally verified the area-rule concept of transonic drag[6] that the foundation was laid for the integrated design of supersonic aircraft. An earlier and virtually unknown work by Hayes,[7] was found to provide the mathematical basis for this fundamental far-field concept. Subsequent work by Jones and others,[8] for example, produced the first early procedures for calculating the zero-lift wave drag of complete slender configurations at supersonic speeds.

At $M = 1$, the area-rule concept is a classic of simplicity. As illustrated in Fig. 3, a given wing-body configuration is considered to be intercepted by a series of parallel cutting planes normal to the aircraft axis. The resulting cross-section areas are then converted to equivalent area circles which, in turn, define an equivalent body of revolution. The area-rule concept of Whitcomb states that the wave drag of the equivalent body is the same as that of the complete configuration at $M = 1$.

For supersonic speeds, however, the problem becomes more complex. The more general far-field theory of Hayes and Jones requires that the parallel cutting planes be tangent to the Mach cone with the intercepted areas projected onto a plane normal to the aircraft axis. Now there is no longer a single equivalent body. For each Mach number, there exists a series of equivalent bodies—one for each of the many roll angles of which only two are shown on the sketch. The wave drag of the complete configuration for a given Mach number is the integrated average of the equivalent-body wave drags through the full roll range of 360°.

The problem of determining the configuration cross-section areas and their equivalent bodies can be time consuming, but here is where the high-speed electronic computer pays off. The Boeing Company in the early 1960's developed a digital-computer program, subsequently adapted at NASA-Langley,[9] which applied the equivalent-body theoretical approach to the solution of aircraft wave drag. The numerical description of the complex configuration (see Fig. 4) was accomplished by systematic specification of fuselage and nacelle radii along with wing- and tail-surface reference points, with the assumption of linear contours between successive ordinates. More recently, improvements have been made in the numerical

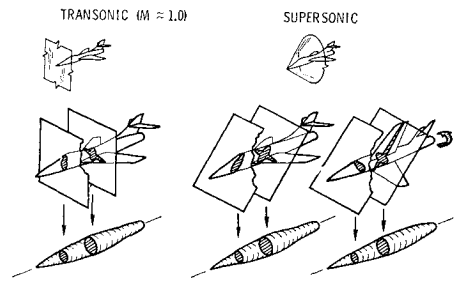

Fig. 3 Illustration of area rule.

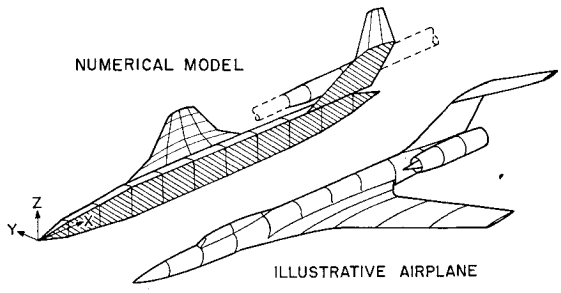

Fig. 4 Numerical representation of illustrative airplane for machine-computing procedure.

description of an airplane such that more complex configurations can be described. Figure 5 shows two computer-generated drawings of a high-wing fighter airplane. In the upper half of the figure, the numerical model that would have been used with the original program limitations is shown. The lower half of the figure shows the revised numerical model. By using automatic digitizing equipment, the refined numerical model can be generated in card-deck form in a few hours. Once the aircraft description is stored in the memory unit of the computer, the area distributions of the equivalent bodies are determined by geometric solutions for the normal projection of the areas intercepted by the cutting planes. Computer calculation of wave drag for the resulting equivalent bodies can be evaluated by any one of several methods (Von Kárman,[4] Eminton and Lord,[10,11] and others).

A comparison of machine-computed wave-drag coefficients with wind-tunnel experiment is shown in Fig. 6 for several complete airplane configurations. The experimental drag coefficients that cover a Mach range from 1.4 to 3.2, were obtained by subtracting from the measured zero-lift drag a theoretical estimate of the skin-friction and camber-drag (drag-due-to-lift at zero net lift) components. Except for two cases, the computed wave drag is seen to agree very well with the experimental wave-drag results. It should be noted that the correlation covers equivalent body fineness ratios as low as 8, and that far-field theory can provide reliable wave-drag estimates—even down to the relatively low fineness ratios examined.

A significant advance in wave-drag optimization procedures has been made recently by Harris at Langley. A numerical technique for the direct solution of the fuselage that is required for a complete configuration to have minimum wave drag has been developed and programed for the computer. It can be shown that the wave drag of a complete configuration is minimum when the average of all the many equivalent bodies has a minimum wave-drag shape. The mathematical basis for this theoretical approach was first published by Ward in 1955.[12] However, as with many theoretical approaches, it has been the development of numerical solutions applicable to the high-speed digital computer which has made a practical tool of the theory.

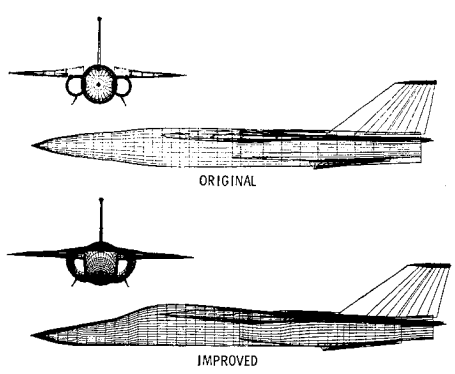

Fig. 5 Examples of numerical models.

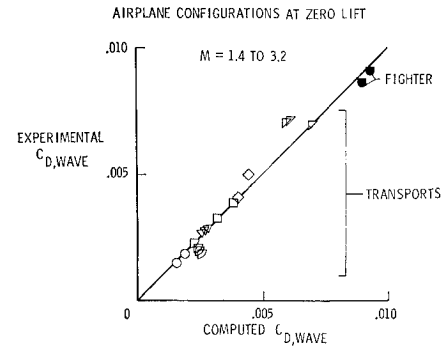

Fig. 6 Machine-computed wave drag vs experiment.

The numerical technique that has been programed is illustrated in Fig. 7. The plot on the left of the figure shows as a solid line the average equivalent body area distribution for a typical complete airplane configuration with a cylindrical fuselage. The sketch on the right shows the fuselage normal area distribution as a solid line. Any number of arbitrary restraint points, illustrated by the solid symbols, may be specified. The computer locates the restraint points on the average equivalent body area distribution for the complete configuration and then solves for the minimum wave-drag shape through the restraint points. The shaded region represents the area which must then be added or subtracted from the original fuselage to define the fuselage for minimum wave drag.

Figure 8 shows as an example some calculated results for the typical configuration. The dashed line represents the lower bound of the configuration wave drag with the three fuselage restraint-points illustrated in the previous figure. For comparison purposes, the wave-drag variation with Mach number is also shown for the configuration with the original cylindrical fuselage, and the $M = 1.5$ and $M = 2.5$ optimum fuselages.

Lifting-Surface Theory

Research on lifting-surface theory dates back to the 1940's where limited success was attained in predicting general wing-alone characteristics at supersonic speeds,[1] for example. In the area of drag minimization, substantial effort was devoted to realizing the favorable characteristics predicted by linear theory for arrow wings having subsonic leading edges—that is, leading edges swept behind the Mach cone from the wing apex. Theoretical studies progressed from the flat wing to an optimum warped surface, but early experiments were largely unsuccessful in realizing the favorable drag-due-to lift potentials. A brief summary of the state-of-the-art as of a decade ago is given by Brown and McLean.[13]

The concept of a restricted optimum lifting surface was proposed by Brown and McLean as a means for limiting theoretical pressures and surface slopes to levels which the flow could reasonably be expected to tolerate without separation. Carlson demonstrated that a substantial portion of the optimum theoretical benefits could be experimentally

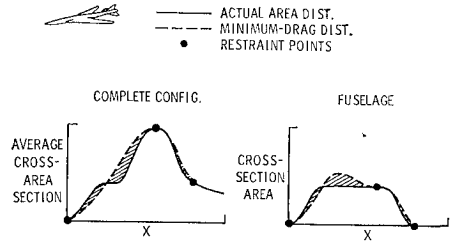

Fig. 7 Direct solution for optimum fuselage for wave-drag minimization.

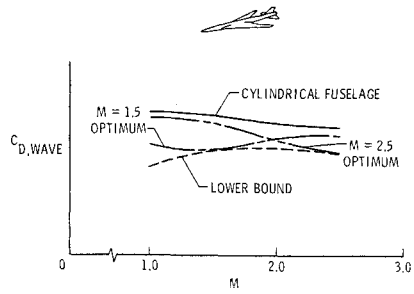

Fig. 8 Effects of fuselage optimization on wave drag.

realized—at least for the lower design lift coefficients—and that sizeable self-trimming moments would also result.[14]

Early research in supersonic drag-due-to-lift and lifting-surface theory was hampered by the difficulties in designing and constructing the complex wing surfaces called for by theory and in assessing the effects of changes in wing surface which are dictated by practical considerations (e.g., fairing out of the theoretical surface discontinuity at the wing root). This roadblock was lifted by the development by Carlson and Middleton[15,16] of numerical techniques which permitted the rapid design and evaluation of wings of arbitrary planform and surface slope. Figure 9 illustrates the representation of a wing in the numerical analysis. Linear theory provides a solution for the lifting characteristics of an element in the flowfield created by one or more forward elements. A wing half panel may be represented as an array of elements (usually 500–1000 in number) wherein the surface slopes are specified and the resulting lifting pressures calculated by following a precise routine from front to rear. This numerical procedure has been programed for high-speed computers and has become a most valuable aerodynamic tool.

The capability for calculating directly the loading distribution for arbitrary warped planforms has opened up new aerodynamic design horizons. Now the calculated drag-due-to-lift penalties for "restricted" surface loadings, wing centerline fairing, or C_{m0} specification can be systematically assessed and compared with experiment. Figure 10 presents a comparison of experiment and theory at $M = 2$ for arrow wings having a flat and a warped surface. The drag correlation is noted to be excellent. The pitching-moment correlation is adequate at low lifts; however, it breaks down at the higher values of C_L. Note for the design C_L, only a small drag penalty is paid for fairing out the infinite incidence at the root chord. Of particular importance is the self-trimming characteristics of the warped wing provided by the large positive pitching moment at zero lift. This theoretical capability to predict wing-alone lift and moment characteristics, in combination with the zero-lift wave-drag programs discussed previously, provides the cornerstone for the design integration of supersonic aricraft.

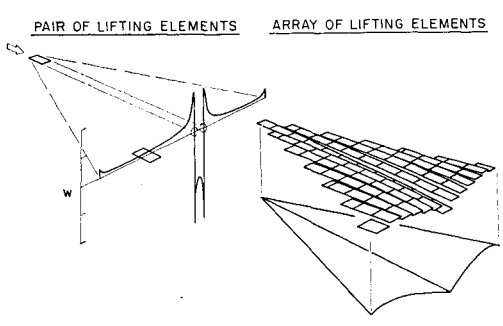

Fig. 9 Lifting-surface representation for machine-computing procedure.

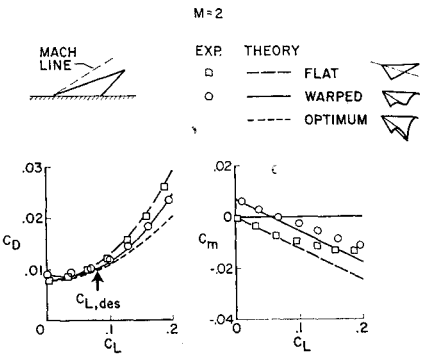

Fig. 10 An example of the use of wing warp.

Wing-Body Integration

The technology for integration of the wing and body into a near-optimum configuration is based on the previously discussed fundamental theoretical concepts and is anchored by key experimental results. For zero-lift conditions, the wave-drag program accounts for the wing-body interference effects due to component thickness; however, wing-body lift interference effects are more complex. Figure 11 presents some key experimental results by Carlson[17] which demonstrated that the most efficient wing-body configuration results when the fuselage is alined with the wing root camber line. The conclusion that can be drawn from these results is that the optimum body configuration for the lifting condition should entail a minimum change in the optimized loading distribution selected for the wing alone. This general conclusion for slender configurations will have application later when integration of the wing and nacelle is under consideration.

An approximation of wing-body lift interference effects can be made by including the fuselage as a part of the planform in establishing the mean camber surface. However, when the fuselage is displaced vertically and is large compared to the wing (as in a typical fighter aircraft or missile configuration) significant lift-volume interactions can exist. Harris has applied Hayes' concepts as an extension to the existing wave-drag programs to account for lift-volume interference effects.[18]

Stability and Trim Effects

Recent extensions have been made to the basic lifting-surface programs to include the effects of a horizontal tail or canard surface (see Fig. 12). The heavy dashed lines illustrate the planform that is input to the computer. The cross-hatched areas are specified as regions which can carry no load. The planform is divided into a matrix of panels, and the computer calculates the loading for each panel which is on the physical planform. A basic assumption of the present technique is that the vertical displacement between panels is small and can be neglected.

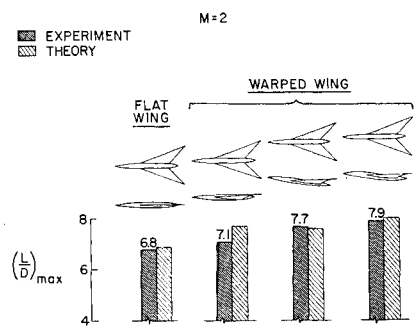

Fig. 11 Effects of fuselage alignment.

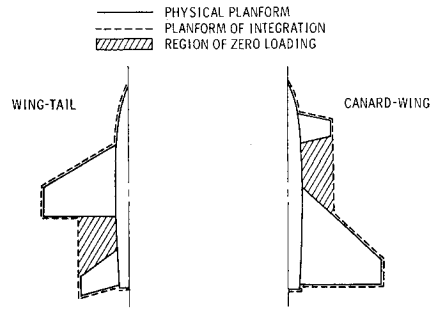

Fig. 12 Application of lifting-surface theory to discontinuous planforms.

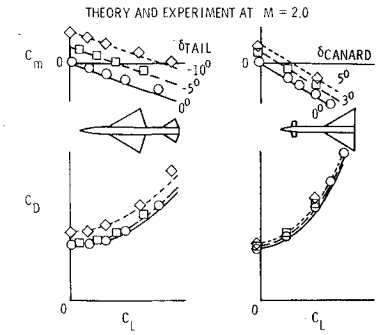

Fig. 13 Prediction of stability and control effects.

Figure 13 shows some comparisons between theory and experiment at a Mach number of 2.0. The drag and moment characteristics for a fighter configuration with the horizontal tail deflected 0, −5, and −10° are shown on the left of the figure. A similar comparison is shown on the right of the figure for a configuration with three deflection angles of the canard surface. The agreement between theory and experiment is quite good for both configurations, particularly at the lower lift coefficients. For configurations which have large vertical displacements of the mean camber surface (which includes the wing, body, and tail), the agreement is not as good as that shown here. Analytical effort is now underway in this area.

Another recent addition to the lifting-surface programs provides for optimization of the wing camber surface in the presence of interference flowfields—as, for example, engine nacelles located in proximity of the wing. Mack[19] has recently programed a numerical procedure for determining the wing slope changes required to remove various fractions of the interference lift and has assessed the resulting increments of lift-induced drag and C_{m0}.

Complex of Computer Programs

A numerical model of the configuration is the key element in the complex and serves as the starting point for all programs. The availability of a numerical model stored in the computer provides the capability for computer-generated drawings to serve as a check on human input errors (for example, see Fig. 5). Refinement of the numerical model is an iterative process, and as the configuration evolves, progressively more precise model definition can be made.

Once the numerical model of a configuration has been specified to the computer in sufficient detail, it becomes a relatively simple step for the computer to strip out component surface wetted areas and reference lengths. With the specification of flight Mach- and Reynolds-number conditions, the surface skin-friction drag can be calculated taking into account form factors, cutoff Reynolds number, surface roughness, mixed laminar/turbulent flows, heat transfer, and so forth.

The complex or operational Langley computer programs showing the sources of input data and the recipient of the output data is presented as a flow diagram in Fig. 14. In the interests of simplicity, the various subprograms are not shown. In the synthesis of a new design, an iterative process is necessarily involved in obtaining the desired performance. The output of these various programs comprises the theoretical aerodynamic characteristics which are then used as input data to the mission analysis programs. Note that these analytical programs provide the basic ingredients for evaluation of the configuration sonic-boom characteristics as well.[20,21]

An alternate to the purely analytical route is the wind-tunnel route to provide experimental aerodynamic characteristics. This route is relatively straightforward except for one area of concern—the extrapolation of wind-tunnel data to full-scale flight conditions. The resulting analysis is comparable in scope to that required for an independent determination of the full-scale theoretical aerodynamic characteristics. In the wind-tunnel process, the theoretical characteristics of the model under its test conditions are evaluated by the complex of computer programs for comparison with the experimental wind-tunnel results. Experimental/theoretical correlation must be established at this stage as a prerequisite to a valid process. The next step in the process is to determine by direct computation and analysis the predicted full-scale aerodynamic characteristics of the flight vehicle. This involves consideration of skin friction at cruise Reynolds number, aircraft surface finish and protuberances, jet exhaust effects, and differences between model and prototype (e.g., fuselage closure), and so forth. The so-called "extrapolation" increment is the difference between the computed model and full-scale estimates. Brown and Chen[22] discuss the probable accuracy of this total procedure and conclude that the accuracy of these experimental/analytical ground-based procedures can be equivalent to the experimental accuracies expected to be obtained from carefully controlled flight tests.

Applicability of Analytical Procedures

The key analytical procedures noted in the previous sections had their first critical test in 1965 when they were applied by FAA/NASA to the aerodynamic evaluation of the supersonic transport designs. Critical wind-tunnel tests were performed by the manufactures and the NASA, and these results were correlated with theory. A typical comparison of theoretical and experimental untrimmed drag polars for the two SST models at wind-tunnel test conditions for the cruise Mach number of 2.7 is illustrated in Fig. 15. Although some discrepancies between experiment and theory are observed, in the critical region near L/D_{max} excellent agreement is noted. The observed drag discrepancy was about two counts (0.0002) at cruise C_L, which approaches the level of wind-tunnel experimental accuracy. Similar correlations between theory

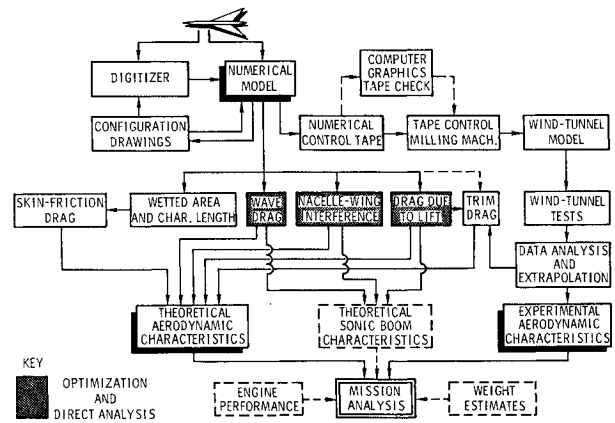

Fig. 14 Complex of computer programs for supersonic aircraft design and evaluation.

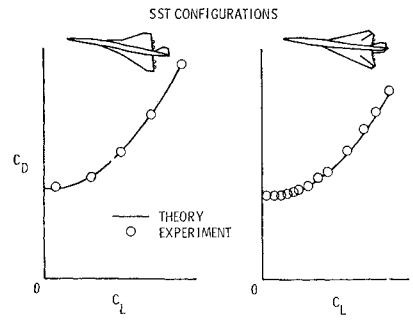

Fig. 15 Comparisons of theory and wind-tunnel experiment at $M = 2.7$.

and experiment were observed for the lift-drag polars down to a Mach number of about 1.4.

For configurations that are not as slender as the SST models and which violate the assumption of small vertical displacement in the mean camber surface, the agreement is not as good. The high-wing fighter aircraft shown in Fig. 16 is an example of a configuration that violates both of these theoretical restrictions. Comparisons of theory and experiment for a wind-tunnel model of the representative fighter configuration at Mach numbers of 1.6 and 2.2 are shown in the figure. Although the agreement for fighter-type configurations is generally not as good as that for the more slender SST configurations, the agreement is usually as good, if not better, than the example shown here. This level of agreement is considered to be adequate for preliminary design studies.

The applicability of this new supersonic technology, however, is not limited to its use as an evaluation procedure. The power lies in its use as an aerodynamic design tool. No longer need the harried designer base his supersonic performance estimates and trade studies on empirical relations or aerodynamic data of questionable applicability. Instead, in a matter of hours, a skilled aerodynamicist can calculate the supersonic performance characteristics of a specified configuration and systematically assess the effects of various trades, such as engine-pod location, fuselage volume distribution, or changes in wing thickness. With this available technology base, the long lead-time wind-tunnel tests can be reserved for an over-all configuration check, or for securing detailed information of stability and control characteristics, inlet-exit flowfields, store drag and separation characteristics, and so forth. The wind tunnel and analytical programs handled in this fashion complement each other and provide effective and timely data during the preliminary design cycle.

Illustrative Application to High Performance SST

Loftin[23] has considered the basic elements in the design integration of a supersonic transport configuration having L/D_{max} approaching 10 at cruise speed near $M = 3$. This has been the goal of aerodynamicists for the past decade. Attainment of such a level of cruise efficiency in a vehicle configuration having a low structural-weight fraction, as well as meeting flight off-design and airport operational requirements, could assure the economic feasibility of the supersonic transport. In the remaining portion of the paper, we shall endeavor to illustrate the detailed aerodynamic considerations and processes involved in the initial aerodynamic cycle of a high aerodynamic efficiency supersonic transport.

To simplify this illustrative procedure, two basic constraints must be recognized. First, the primary design consideration will be the attainment of maximum cruise lift-to-drag ratio at $M = 2.7$. Since every element of the design must provide for optimum lifting efficiency with a minimum of drag, the resulting configuration logically will tend toward an integrated flying wing or tailless configuration having a minimum wetted-to-wing area ratio. The starting point for the design process will be selected on the basis of a background of experience to preclude blind alleys or reiterative cycles which are characteristics of a real-lift design process. Second, only limited consideration will be given to the necessary off-design aerodynamics, or to structural, propulsion, and operational considerations. Typical constraints of the supersonic transport will be introduced to illustrate the technology application; however, a complete aerodynamic design integration can be accomplished only by a competent aircraft design team after considerable study in depth.

The key starting assumptions are cruise at $M = 2.7$ and 62,500-ft altitude, 675,000-lb takeoff gross weight, 10,000-ft^2 (approx.) wing area, 200 passengers plus 350,000-lb fuel in the wing.

Wing Selection

The wing provides the lift as well as the pitching moment for cruise trim. It also establishes the drag-due-to-lift factor and produces the major component of the wave drag and skin friction. Since all elements other than the wing—that s, fuselage, nacelles, and stabilizing surfaces—only tend to degrade the basic wing potential, it is obvious that the wing selection must dominate the design.

The planform of the wing essentially determines the drag-due-to-lift as well as the wave-drag characteristics of the wing. Figure 17 summarizes for $M = 2.7$ the linear-theory optimum drag-due-to-lift factor as a function of leading-edge sweep angle and for various trailing-edge notch ratios. As is well known, the lowest drag-due-to-lift factor occurs when the leading edge is swept well behind the Mach line and the trailing-edge notch ratio is maximized. Figure 18 shows, however, that there are many important factors other than pure supersonic efficiency to consider in selecting the best over-all planform. The factors of subsonic L/D, pitching-moment linearity, ride quality, and structural efficiency—to name only a few—are important in planform selection. For the purposes of this illustrative example, a leading-edge sweep of 74° and a trailing-edge notch ratio of approximately 0.3 has been selected for the initial aerodynamic cycle. The potential L/D_{max} for a zero-thickness wing of the selected planform for all turbulent flow at full-scale Reynolds number is 14.5. This provides a modest, but perhaps adequate, cushion to reach our aerodynamic design goal of $L/D_{max} \simeq 10$ for the complete configuration.

A pointed-tip arrow wing leaves something to be desired from the standpoint of local aerodynamic flows as well as structural considerations. Figure 19 suggests various detailed adjustments to the basic planform which warrant consideration. A clipped tip will decrease the structural span and eliminate that portion of the wing where experiment has

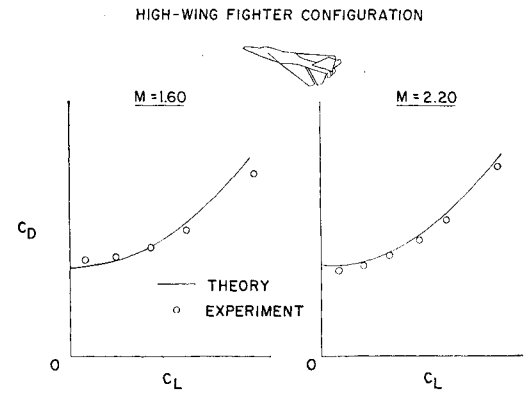

Fig. 16 Comparisons of theory and wind-tunnel experiment at $M = 1.6$ and 2.2.

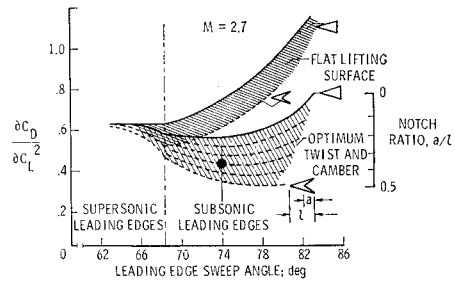

Fig. 17 Drag-rise factors for arrow wings.

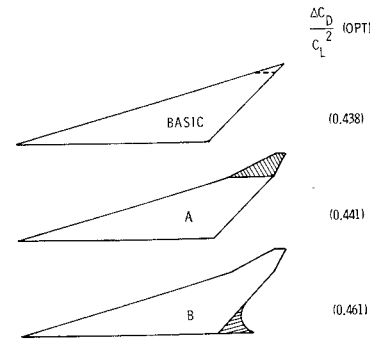

Fig. 19 Detailed wing planform modifications.

indicated a breakdown of the theoretically-predicted flow. Unsweeping the wing tip in the region of high local upwash (Planform A) will improve the subsonic efficiency and diminish pitch nonlinearities with little detriment to the supersonic drag factor. Planform B, which fills in a portion of the trailing-edge notch near the fuselage, is suggested by considerations of additional improvement in subsonic pitching-moment linearity, trailing-edge flap effectiveness, and efficient thickening of the wing root for volume and structural weight benefits. The computer-derived optimum drag-due-to-lift factor for Planform B is 0.461 compared to a value of 0.438 for the reference arrow planform. This increase in drag factor (5%) is modest and would appear justified, but the effectiveness of these planform adjustments from an over-all configuration standpoint cannot be determined without an integrated design study in depth. For the purposes of this illustrative example, however, Planform B will be carried through the design cycle.

Camber Surface Design

The design C_L for the specified cruise conditions is 0.085 for an assumed weight at start of cruise of approximately 600,000 lb. Figure 20 presents some practical restraints to the optimum camber surface for Planform B. The first provides for a practicable fairing out of the centerline wing discontinuity of the optimum camber surface. Prescribing the revised camber surface to the inverse drag-due-to-lift program results in a value of $\Delta C_D/C_L{}^2$ of 0.486, which represents an additional 5% penalty. This compares to a reference flat-plate drag factor of 0.655 for Planform B.

The camber surface can also be adjusted to provide a center of pressure location other than that resulting from the specified camber surface. This can be accomplished by a trial and error process between the inverse and direct solution camber programs to establish a minimum drag penalty for a given center of pressure shift. Also, noted on Fig. 20 is provision for vertical shearing of the chordwise wing stations to improve the lines of the leading and trailing edges or to provide for straight-line hinging of control surfaces. Within the limitation of the theory, no drag penalty for modest vertical shearing would be anticipated.

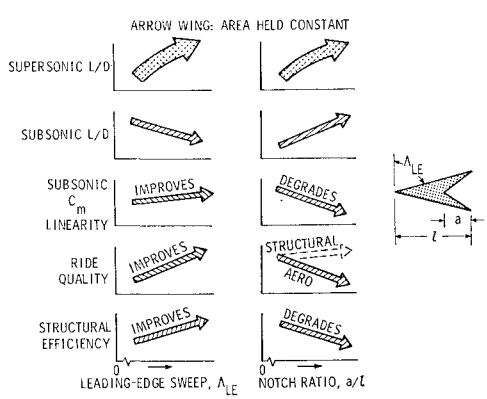

Fig. 18 Effects of leading-edge sweep and notch ratio.

Airfoil Section

The thickness ratio of the wing is constrained by considerations of wave drag, structural weight, and wing volume for fuel and the landing gear. A wing thickness ratio of $2\frac{3}{4}\%$ provides about a 57-in. wing depth at the fuselage side, which appears adequate for landing gear stowage. Since a rounded leading edge can be utilized where the Mach line lies well ahead of the leading edge, a modified NACA 65-series section will be selected to improve subsonic performance characteristics. A check on wing volume shows a total of 17,000 ft^3. Usable volume of 10-in. depth or greater is found to be 13,200. Since 7000 ft^3 (350,000 lb) is required for wing fuel, it is evident that the assumed wing is not volume limited.

A check on the wing-alone potential L/D_{max} for the prescribed $2\frac{3}{4}\%$ thickness sections produces a value of 11.8, compared to the zero thickness value of 14.5. When detailed wing design trades are made, it may be found that changes in spanwise thickness ratio or location of section maximum thickness may be desired. These all can be evaluated by appropriate changes in the numerical model.

Nacelle Design and Location

The general problem of propulsion system integration for supersonic aircraft has been analyzed in considerable depth by Nichols[24] and it is shown to impact on almost every element of airframe design. Robins[25] and Sigalla[26] have analyzed the detailed nacelle design and location for optimum cruise efficiency. The total integration problem is far more complex than can be considered here, but some general conclusions can be drawn. From considerations of drag, jet-exit efficiency, favorable effects on directional stability, and so forth, the most efficient arrangement consists of podded nacelles located under the wing and behind the line of wing maximum thickness. The effectiveness of various detailed nacelle locations—which may be constrained by considerations of wing structure, adjacent inlet shock interference, jet impingement, of trailing-edge control surface arrangement—can be evaluated from a zero-lift wave-drag standpoint by present programs as illustrated in Fig. 21. On the basis of such an

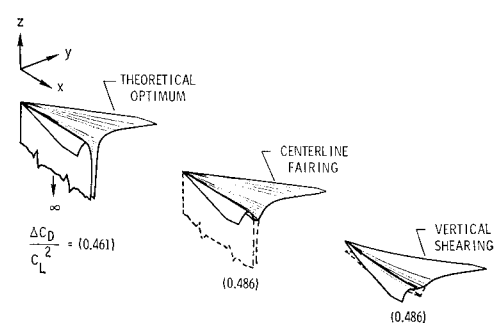

Fig. 20 Wing camber surface definition.

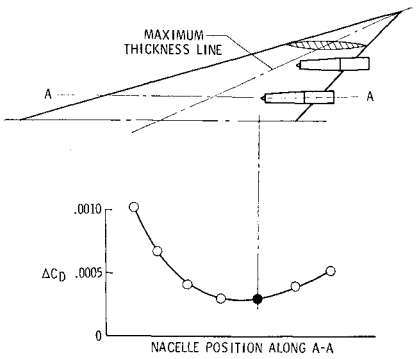

Fig. 21 Effects of nacelle position on wave drag.

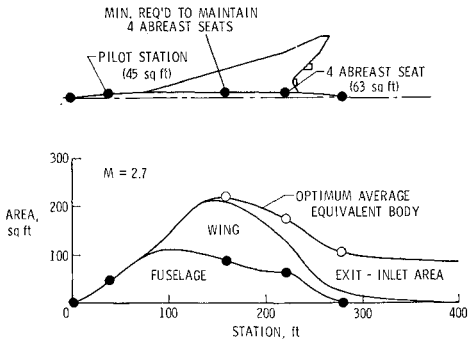

Fig. 24 Fuselage optimization procedure.

analysis, the nacelle location corresponding to the solid point has been selected. The nacelle shape is assumed to correspond to a fully expanded nozzle to maximize nozzle and and boat tail efficiency at cruise conditions.

Landrum[27] has shown that nacelle alignment can also have an influence on the drag. As illustrated in Fig. 22, a nacelle-pylon installation experiences a side force because of the local sidewash produced by the lifting wing, and a component of this force acts in the drag direction. It is interesting to note that when the nacelle cant angle is between the free-stream and the local flow angle, the side force produces a negative drag, or thrust component. Experimental results,

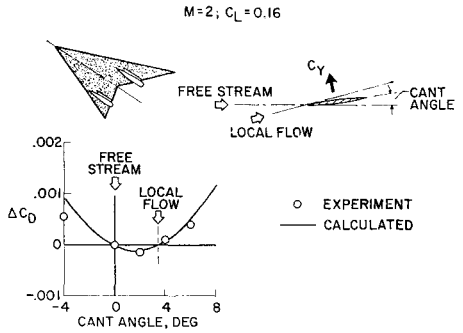

Fig. 22 Effects of nacelle alignment.

as well as calculations, indicate that the thrust force is maximum when the cant angle is one-half the local flow angle. Therefore, calculations were made to determine the local flow angles at the nacelle positions and each nacelle was aligned at one-half the local sidewash angle (0.75° for the inboard nacelle and 1.75° for the outboard nacelle).

Wing Reflex in Presence of Nacelles

As noted in the section on lifting-surface theory, the optimum lifting efficiency is attained when there is a minimum change from the optimum loading distribution selected for the wing alone. This is especially true for the case of nacelles

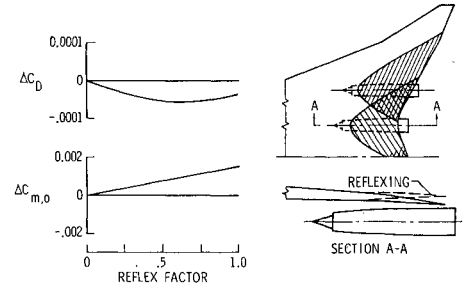

Fig. 23 Wing reflex interference optimization.

located under the trailing edge of the wing, for not only can the lifting efficiency be reduced, but the generation of large positive interference pressures under the wing near the trailing edge will produce large nose-down pitching moments. Thus, it is recommended in the noted references that the wing be reflexed in the region of nacelle influence as shown in Fig. 23 to relieve the wing of the nacelle interference lift. The program of Mack[19] supplies the reflex ordinates as well as the lift-induced drag and C_{m_0} increments as a function of reflex factor—the fraction of interference lift removed. A reflexed surface which cancels $\frac{2}{3}$ of the nacelle interference load for cruise conditions has been chosen for this design study.

Fuselage Design

With the wing-nacelle combination established for this first cycle analysis, the fuselage is the only major component remaining to be integrated into the complete configuration. The fuselage aerodynamic requirement can be easily stated—to provide a specified internal volume for a minimum in total configuration drag at cruise conditions. The determination of the optimum longitudinal area distribution under prescribed restraints no longer is an iterative process, for it can be solved for directly by using Harris' procedure discussed previously. Figure 24 notes the various fuselage control points, the optimum average equivalent body area distribution encompassing these points, and the resultant fuselage areas and contours. The effect of any given control point restraint can be determined by dropping that point from the optimization procedure and assessing the resulting effect on fuselage shape and drag. The zero-lift wave drag of the complete wing-body nacelle configuration (Fig. 24) is determined to be but 12 counts (C_{D_w} = 0.0012), which is approximately equal to that of the basic wing alone.

Still to be specified is the manner in which the fuselage and wing are integrated to maximize L/D ratio. Drag-due-to-lift considerations dictate that the fuselage volume must be added so as to leave essentially unchanged the wing design loading distribution. Thus, the change in cross-section area

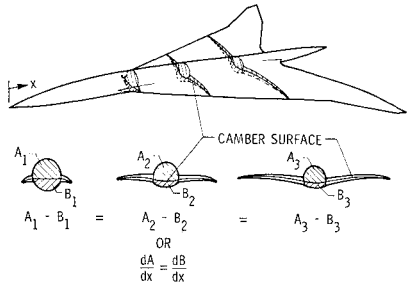

Fig. 25 Fuselage cross-section distribution about camber surface.

Table 1 Theoretical drag at $M = 2.7$

Drag breakdown at $C_L = 0.085$, $(M = 2.7)$	
Wave	0.0012
Friction	0.0037
Lift-induced	0.0035
Propulsion (misc.)	0.0002
Roughness	0.00025
Total	0.00885
$(L/D$ cruise $= 9.6)$; $(L/D_{max} \simeq 9\frac{3}{4})$	

with length (dA/dx) above and below the wing camber surface must be the same for each fuselage station (see Fig. 25). This can be accomplished by a trial and error graphical process working from computer-drawn cross sections. Sections other than circular can be utilized to permit more refined design adjustments (e.g., fuselage lobeing near the passenger and and cargo compartments).

Vertical Tails

The basic aerodynamic definition of the illustrative SST configuration, except for a consideration of the control surfaces, has now been largely set. It will be assumed that longitudinal and lateral control will be obtained by wing trailing-edge flaps, while directional control will be provided by twin vertical tails near the wing tips. Design considerations beyond the scope of this paper will determine optimum control arrangement. The volume effects of the vertical tails on wave drag would have to be evaluated in later cycles.

Since all elements of the configuration must be optimized for the cruise conditions, orientation of the vertical tails from the standpoint of the local sidewash angles also must be considered. This results in about $2\frac{1}{4}°$ of toeout on the outboard vertical tails.

Analysis of the Configuration

The illustrative configuration is now sufficiently defined to determine X-Y-Z numerical model. The input check via computer graphics is shown in Fig. 26. The buildup of the theoretical drag polar at $M = 2.7$ is shown in Fig. 27 and Table 1. Note that the value of L/D_{max} approaches the goal of 10, and for the cruise lift coefficient the configuration is trimmed $(C_m \simeq 0)$.

Although experimental data are not available on this specific illustrative model, wind-tunnel tests of similar configurations have demonstrated a level of accuracy comparable to that shown in Fig. 15. Theoretical drag polars can be calculated through the Mach number range down to about $M = 1.4$, where transonic effects render the results questionable at lower Mach numbers. Brown and Chen[22] assess the over-all statistical accuracy of correlation between wind-tunnel drag predictions and experimental drag values from well instrumented flight tests as $\pm 5\%$.

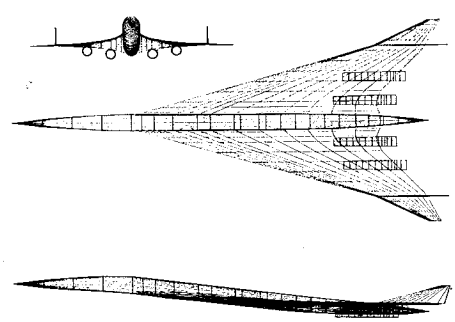

Fig. 26 Computer-generated drawing of SST configuration.

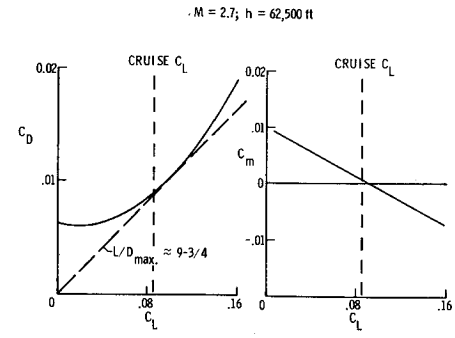

Fig. 27 Theoretical characteristics of the complete configuration.

Concluding Statement

It should be evident from the preceding presentation that the supersonic technology of a decade ago—largely through theory extension and ingenious use of the high-speed computer—has been forged into a powerful design tool which can provide hard aerodynamic inputs early in the design cycle. This advanced technology has direct application to the supersonic transport, advanced military aircraft, and missiles. Effective utilization of this advanced aerodynamic technology, however, requires a word of caution. The complex of computer programs considered in this paper is merely a tool available to the designer. And like any complex tool, there must be complete understanding of its capability and limitations backed by critical operational use. The key staff members immediately responsible for application of this program technology must be highly skilled but can be small in number—perhaps no more than a half dozen. The effective training of this key group will be long and arduous, but there is no alternative to the continual exercise of the various programs and checking against experiment until every limitation and every capability are fully understood. Then, and not until then, can these programs be used with confidence and imagination.

An equally important point to be made is the stage at which the computer programs are introduced into the design process. The answer is the sooner the better—even the back-of-the-envelope designs should consider area distributions, effective camber surfaces, center-of-pressure control, and the like. The complex of computer programs should be utilized at every possible stage to guide the evolving design toward the performance goal. The great potential of this advanced technology will be lost if it is used only for evaluation after the design already has been largely frozen. The resulting performance surprises may be too late to correct. But in the hands of a competent design staff, the advanced technology presented here can revolutionize the aerodynamic design of present and future supersonic aircraft and lead the way to new levels of performance and efficiency.

References

[1] Brown, C. E., "Theoretical Lift and Drag of Thin Triangular Wings at Supersonic Speeds," Rept. 839, 1946, NACA (supersedes NACA TN 1183).

[2] Woodward, F. A. and Larson, J. W., "A Method of Optimizing Camber Surfaces for Wing-Body Combinations at Supersonic Speeds, Part I—Theory and Application," Doc. D610741, Pt. I, 1965, The Boeing Co., Seattle, Wash.

[3] Charmichael, R. L., "A Critical Evaluation of Methods for Computing Wing-Body Interference at Supersonic Speeds,"; presented at the Sixth Annual Congress of the International Council of the Aeronautical Sciences, Sept. 9–13, 1968, Munich, Germany.

[4] Von Kármán, T., "The Problem of Resistance in Compressible Fluids," Reale Accademia d'Italia, Classe della Scienze Fisiche, Matematiche e Naturali, Quinto Convegno Volta, Rome, 1935, pp. 222–276.

[5] Puckett, A. E., "Supersonic Wave Drag of Thin Airfoils," *Journal of the Aeronautical Sciences*, Vol. 13, No. 9, Sept. 1946, pp. 475–484.

[6] Whitcomb, R. T., "A Study of the Zero-Lift Drag-Rise Characteristics of Wing-Body Combinations Near the Speed or Sound," Rept. 1273, 1956, NACA (supersedes RM L52HO8, Sept. 1952, NACA).

[7] Hayes, W. D., "Linearized Supersonic Flow," Rept. AL-222, June 18, 1947, North American Aviation Inc., Los Angeles, Calif.

[8] Jones, R. T., "Theory of Wing-Body Drag at Supersonic Speeds," Rept. 1284, 1956, NACA (supersedes NACA RM A53H18a).

[9] Harris, R. V., Jr., "An Analysis and Correlation of Aircraft Wave Drag," TM X-947, 1964, NASA.

[10] Eminton, E., "On the Minimization and Numerical Evaluation of Wave Drag," Rept. Aero. 2564, 1955, Royal Aircraft Establishment.

[11] Eminton, E. and Lord, W. T., "Note on the Numerical Evaluation of the Wave Drag of Smooth Slender Bodies Using Optimum Area Distribution for Minimum Wave Drag," *Journal of the Royal Aeronautical Society*, Vol. 60, No. 541, Jan. 1956, pp. 61–63.

[12] Ward, G. N., "The Drag of Source Distributions in Linearized Supersonic Flow," CoA Rept. No. 88, Feb. 1955, College of Aeronautics, Cranfield, England.

[13] Brown, C. E. and McLean, F. E., "The Problem of Obtaining High Lift-Drag Ratios at Supersonic Speeds," *Journal of the Aerospace Sciences*, Vol. 26, No. 5, May 1959, pp. 298–302.

[14] Carlson, H. W., "Aerodynamic Characteristics at Mach Number 2.05 of a Series of Highly Swept Arrow Wings Employing Degrees of Twist and Camber," TM X-332, 1960, NASA.

[15] Carlson, H. W. and Middleton, W. D., "A Numerical Method for the Design of Camber Surfaces of Supersonic Wings With Arbitrary Planforms," TN D-2341, 1964, NASA.

[16] Middleton, W. D. and Carlson, H. W., "Numerical Method of Estimating and Optimizing Supersonic Aerodynamic Characteristics of Arbitrary Planform Wings," *Journal of Aircraft*, Vol. 2, No. 4, July-Aug. 1965, pp. 261–265.

[17] Carlson, H. W., "Longitudinal Aerodynamic Characteristics at Mach Number 2.02 of a Series of Wing-Body Configurations Employing a Cambered and Twisted Arrow Wing," TM X-838, 1963, NASA.

[18] Harris, R. V., Jr., "A Numerical Technique for Analysis of Wave Drag at Lifting Conditions," TN D-3586, 1966, NASA.

[19] Mack, R. J., "A Numerical Method for the Evaluation and Utilization of Supersonic Nacelle-Wing Interference," TN D-5057, 1969, NASA.

[20] Carlson, H. W., Mack, R. J., and Morris, O. A., "Sonic-Boom Pressure-Field Estimation Techniques," *Proceedings of the Sonic Boom Symposium*, The Acoustical Society of America, St. Louis, Mo., Nov. 3, 1965, pp. 510–518.

[21] Carlson, H. W., *Experimental and Analytic Research on Sonic Boom Generation at NASA*, NASA SP-147, April 12, 1967, pp. 9–23.

[22] Brown, C. E. and Chen, C. Fang, "An Analysis of Performance Estimation Methods for Aircraft," Rept. 921, Nov. 1967, NASA.

[23] Loftin, L. K., Jr., "Research Relating to Large Supersonic Cruising Aircraft," AIAA Paper 67-748, Los Angeles, Calif., 1967.

[24] Nichols, M. R., "Aerodynamics of Airframe-Engine Integration of Supersonic Aircraft," TN D-3390, 1966, NASA.

[25] Robins, A. W., Morris, O. A., and Harris, R. V., Jr., "Recent Research Results in the Aerodynamics of Supersonic Vehicles," AIAA Paper 65-717, Los Angeles, Calif., 1965.

[26] Sigalla, A. and Hallstaff, T., "Aerodynamics of Powerplant Installations on Supersonic Aircraft," AIAA Paper 66-665, Colorado Springs, Colo., 1966.

[27] Landrum, E. J., "Effect of Nacelle Orientation on the Aerodynamic Characteristics of an Arrow Wing-Body Configuration at Mach Number 2.03," TN D-3284, 1966, NASA.

SYNOPTIC: An Experimental Evaluation of Exhaust Nozzle/Airframe Interference, W. C. Schnell and D. Migdal, Grumman Aerospace Corp., Bethpage, N.Y., *Journal of Aircraft*, Vol. 7, No. 5, pp. 396–401.

Subsonic and Supersonic Airbreathing Propulsion

Theme

Advanced multimission aircraft possess nozzle boat tail areas that are large compared to the aircraft cross-sectional area. Sophisticated nozzle/aft-fuselage blending is essential so that the potentially high boat tail drag is minimized (especially at subsonic cruise). Therefore, the aim of this research was to determine the significant differences in nozzle/airframe interference drag resulting from various proposed nozzle/fuselage combinations.

Content

A range of nozzle types and installations for a twin-engine supersonic fighter were evaluated. At subsonic, transonic, and supersonic Mach numbers (0.6–1.3 and 2.2) interchangeable variable throat nozzle types were mated to five realistic aft-fuselage shapes. A unique dual force balance system was used to assess the effects of: engine spacing, peripheral blockage, nozzle/fuselage combination, jet area, nozzle pressure ratio, and Mach number on interference drag.

Six contemporary nozzle types were tested in each of the aft-fuselage installations shown in Fig. 1. These nozzles are 1) IRIS—low boat tailed, circular arc, variable area convergent nozzle; 2) C-D IRIS—IRIS with addition of a divergent shroud yielding a supersonic nozzle at afterburning; 3) C-D—variable flap ejector with schedule of exit to throat area; 4) PLUG—variable area plug nozzle with cowl flaps scheduled to throat area; 5) BIDE—Blow-In-Door Ejector with IRIS primary and free floating doors and tail feathers; 6) REF BIDE—a production Blow-In-Door Ejector type with a flapped convergent primary, used as a baseline nozzle.

The fuselage shapes represent two distinct groups. Fuselage faimly F-1, F-2, and F-3 was employed in determining the effect of peripheral blockage at constant engine spacing; F-3, F-4, and F-5, to examine spacing effects with zero blockage.

Figure 2 is composed of five major sections: 1) fixed nose, 2) nonmetric transition pieces, 3) metric fuselages, 4) air supply system and balances, 5) metric nozzles. The combined nonmetric forebody provides a simulated aircraft flowfield up to the metric section. The dual force balance system contains a highly sensitive fuselage drag balance which accurately measures and simultaneously transmits this force to the higher capacity over-all thrust minus drag balance.

Previous work has resulted in determining that interference drag is the key parameter to be optimized in exhaust nozzle testing. Interference drag represents the drag increment (or decrement) of the simulated backend at flight pressure ratios relative to a suitable aerodynamic reference backend (usually a nonrepresentative nozzle type operating at a low flow-thru pressure ratio). By measuring nozzle unbiased reference drag D_{RF} in conjunction with static thrust F_{RF} and backend thrust minus drag $(F\text{-}D)_{BE}$ interference drag is determined. $D_{int} = F_{RF} - D_{RF} - (F\text{-}D)_{BE}$.

Results are illustrated in Fig. 3 for the five fuselages and six nozzles at a high subsonic cruise Mach number (0.8).

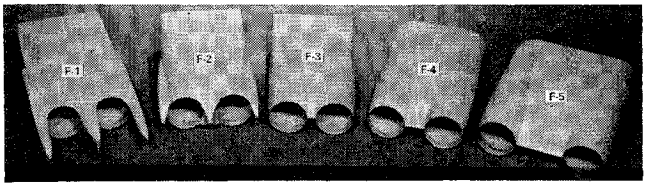

Fig. 1 Aft fuselages.

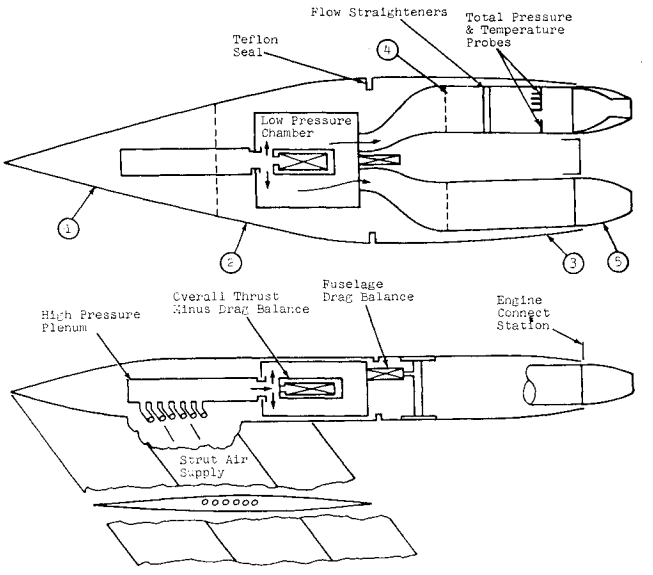

Fig. 2 Model arrangement.

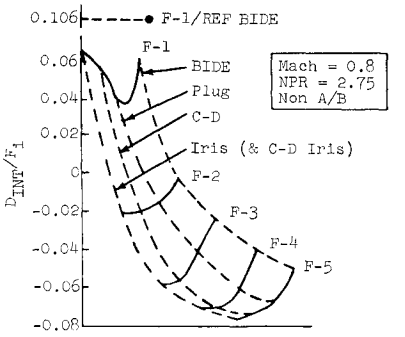

Fig. 3 Subsonic interference drag.

The carpet plot presentation, which is utilized to show the interference drag, indicates the following: 1) The performance of all nozzles becomes highly favorable (negative interference drag) as peripheral blockage is removed. This is observed by following any line of constant nozzle type and noting drag reductions proceeding from F-1 to F-3. The magnitude of these reductions is significant—as much as 12% of ideal thrust or 70 drag counts (assuming $A_{wing} \approx 500$ ft^2). 2) All nozzles incur less drag as spacing ratio increases. Note lines of constant nozzle type proceeding from F-3 to F-5. 3) The closely spaced F-1 type fuselage, featuring a high degree of peripheral blockage, combined with the baseline REF Blow-In-Door Ejector performed significantly poorer than all other configurations. 4) IRIS and C-D IRIS nozzles installed in widely spaced designs, with no peripheral blockage, yield the lowest interference drag.

At maximum afterburning supersonic flight conditions, both 1.2 and 2.2 Mach numbers, the following conclusions are drawn from the test data: 1) The effect of nozzle type is much more pronounced than fuselage installation effects; 2) Nozzle performance continues to improve with reductions in peripheral blockage, although not as significantly as at subsonic cruise conditions; 3) Engine spacing appears to have little effect; 4) Relative to the convergent IRIS, nozzles better suited for supersonic operation such as the C-D IRIS, result in decreased interference drag.